

# MemoAct: Atkinson–Shiffrin-Inspired Memory-Augmented Visuomotor Policy for Robotic Manipulation

Liufan Tan, Jiale Li and Gangshan Jing<sup>†</sup>  
Chongqing University

**Abstract**—Memory-augmented robotic policies are essential in handling memory-dependent tasks. However, existing approaches typically rely on simple observation window extensions, struggling to simultaneously achieve precise task state tracking and robust long-horizon retention. To overcome these challenges, inspired by the Atkinson–Shiffrin memory model, we propose MemoAct, a hierarchical memory-based policy that leverages distinct memory tiers to tackle specific bottlenecks. Specifically, lossless short-term memory ensures precise task state tracking, while compressed long-term memory enables robust long-horizon retention. To enrich the evaluation landscape, we construct MemoryRTBench based on RoboTwin 2.0, specifically tailored to assess policy capabilities in task state tracking and long-horizon retention. Extensive experiments across simulated and real-world scenarios demonstrate that MemoAct achieves superior performance compared to both existing Markovian baselines and history-aware policies. The project page is [available](#).

## I. INTRODUCTION

In recent years, robotic manipulation policies adhering to the Markov assumption have achieved significant progress [1]–[8]. Robots employing this paradigm have demonstrated proficiency in various tasks, such as folding clothes, wiping the table, and making tea. Typically, this learning paradigm predicts a sequence of future actions  $A_{t:t+m-1}$  based solely on the current observation  $O_t$ . However, the assumption that future states depend exclusively on the current moment is ill-suited for memory-dependent tasks [9]–[11], particularly those requiring precise task state tracking and robust long-horizon retention.

Consider the “Sequential Hammer Tap” task shown in Fig. 1 (a) as an example. The robot is required to execute a sequence of sub-tasks: (A) move the left arm with a hammer above the red square, (B) tap the red square, (C) tap the blue square, (D) tap the red square again and stop. Crucially, the observations obtained when tapping the red square are identical, regardless of whether this action occurs before or after tapping the blue square. This perceptual aliasing causes Markovian policies to fail probabilistically [9], [12]–[15], as demonstrated in Fig. 1 (b).

A straightforward approach to address this issue is to expand the observation horizon using a fixed-size window [10], [13], [16], [17]. Algorithms such as [13], [17], [18]

attempt to construct a memory bank based on a First-In-First-Out (FIFO) mechanism. This provides the robot with a degree of historical perception, enabling it to effectively track completed sub-tasks. However, the FIFO update mechanism suffers from a critical limitation: early observations are rapidly displaced by the continuous influx of new data. As a result, historical information beyond the window size becomes inaccessible [9], [12], which causes the model to lose its long-horizon retention capability. In the final sub-task D, the robot quickly loses the memory of having already tapped the blue block, leading it to erroneously repeat the sub-task C, as illustrated in Fig. 1 (b). Furthermore, some other manipulation tasks require recalling the object’s initial state, which is challenging for FIFO-based mechanisms to retrieve due to the temporal distance. Alternatively, MemoryVLA [10] introduces a memory update mechanism that merges the most similar adjacent tokens, allowing for extended long-horizon retention. While this enhances the robot’s long-term memory capabilities, the merging process often discards fine-grained details essential for task state tracking. As illustrated in Fig. 1(b), this can cause the robot to skip sub-task B and prematurely execute sub-task C. Motivated by these observations, a natural question arises: could integrating a lossless memory bank with a lossy long-term memory bank endow robots with simultaneous capabilities for precise task state tracking and robust long-horizon retention?

To answer this question, we draw inspiration from cognitive science, which suggests that memory operates across multiple levels of abstraction [19]–[21]. Specifically, the Atkinson–Shiffrin model categorizes human memory into three distinct tiers: sensory memory, short-term memory, and long-term memory [19]–[21]. Sensory memory encodes the immediate perception of transient events; short-term memory serves as a temporary workspace for retaining recent salient information; and long-term memory acts as a compressed repository preserving experiences accumulated from the distant past.

Guided by this hierarchical cognitive mechanism, we propose MemoAct (Fig. 1 (c)) to explicitly address our initial question. MemoAct comprises three core components: (1) a sensory distillation module that extracts essential sensory memory from redundant visual inputs via a learnable query token; (2) a long short-term memory module that maintains both a lossless short-term memory bank for tracking recent task flows and

<sup>†</sup>Corresponding author.

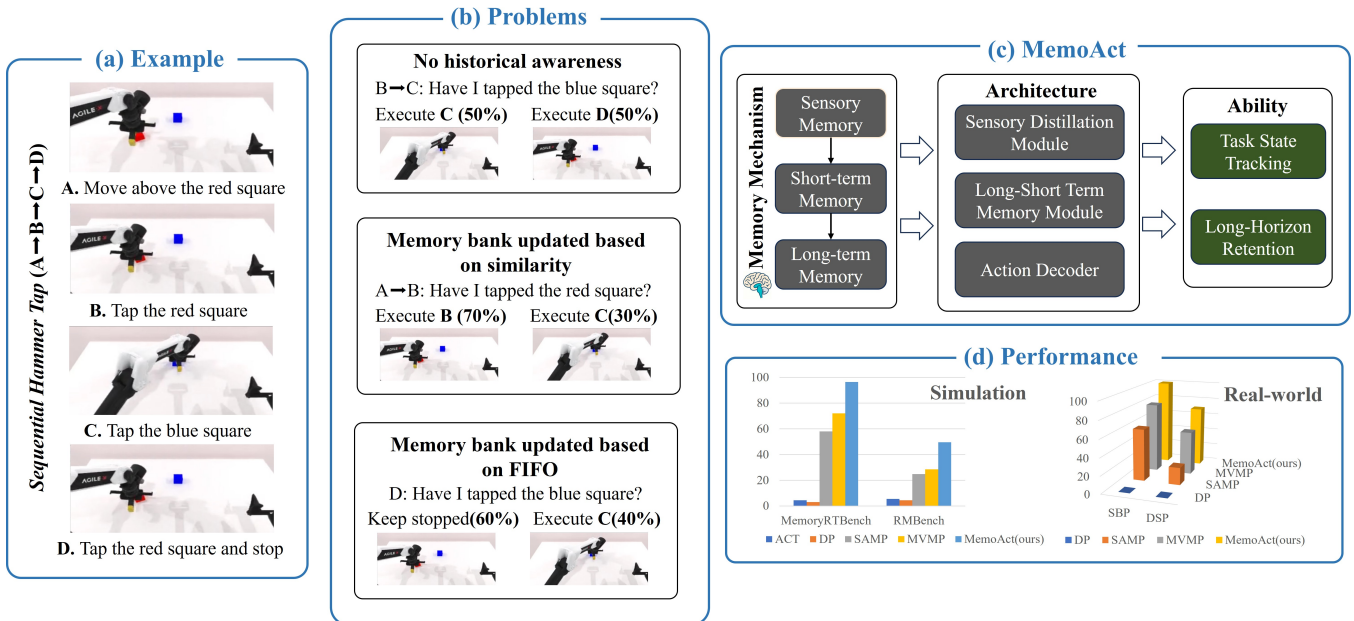


Fig. 1: (a) An example of a memory-dependent task. (b) Policies lacking historical awareness fail under identical observations, while existing representative memory mechanisms suffer from limited long-horizon retention and poor task state tracking. (c) Inspired by the Atkinson–Shiffrin memory model, we propose MemoAct, which simultaneously enables precise task state tracking and robust long-horizon retention. (d) Results on MemoryRTBench, RMBench and real-world experiments demonstrate that MemoAct significantly outperforms baseline algorithms.

a compressed long-term memory bank for encoding persistent historical information through causal attention-based compression and similarity-based merging; and (3) an action decoder that generates history-aware actions based on these memory-augmented tokens.

To systematically evaluate the efficacy of MemoAct, we establish MemoryRTBench, a specialized benchmark derived from RoboTwin 2.0 [22], tailored for assessing robotic capabilities in task state tracking and long-horizon retention. Through comprehensive evaluations across the MemoryRTBench and RMBench [23], as well as in real-world scenarios, we validate MemoAct’s significant superiority over both current Markovian baselines and history-aware policies. Furthermore, comprehensive ablation studies elucidate the distinct contributions of the short- and long-term memory, and we demonstrate the framework’s versatility by seamlessly adapting the memory module to point cloud-based policy baselines.

In summary, our key contributions are threefold:

1) We present MemoAct, a novel robotic policy inspired by the Atkinson–Shiffrin memory model. By leveraging hierarchical memory, MemoAct effectively overcomes the limitations of simple observation window extensions in memory-dependent tasks.

2) We propose a tailored memory update mechanism to maintain the hierarchical memory. This mechanism synergizes a fixed-size lossless short-term bank for precise task state tracking, and a compressed long-term bank for robust long-horizon retention via causal attention-based compression and similarity-based merging.

3) We establish MemoryRTBench, a specialized benchmark for evaluating task state tracking and long-horizon retention. Extensive simulation and real-world experiments demonstrate MemoAct’s advanced performance and its versatile plug-and-play adaptability to diverse policy frameworks.

## II. RELATED WORKS

### A. Advancements in Robotic Manipulation Policies

Recent works have greatly advanced the development of robot policies. [24]–[26]. Architecturally, RT-2 [6] and OpenVLA [7] adopt an autoregressive paradigm by discretizing continuous actions into tokens, while models like  $\pi_{0.6}^*$  and RDT [27] employ diffusion-based heads to generate actions via denoising. To further enhance robustness, MBA [28] and CoT-VLA [29] incorporate future-aware conditioning, utilizing object trajectories and video frames, respectively. Beyond supervised fine-tuning, Reinforcement Learning (RL) has been integrated to enable continuous policy improvement. For instance, SimpleVLA [8] employs RL to optimize strategies directly through environment interaction, whereas WMPO [30] leverages a pixel-space generative world model to bypass the constraints of physical interaction. While these approaches successfully incorporate structured information or efficient architectures to achieve versatility across various scenarios, they struggle to address memory-dependent tasks [9], [10], [12], [23]. There is a pressing need to accelerate research toward endowing robots with robust historical perception capabilities.

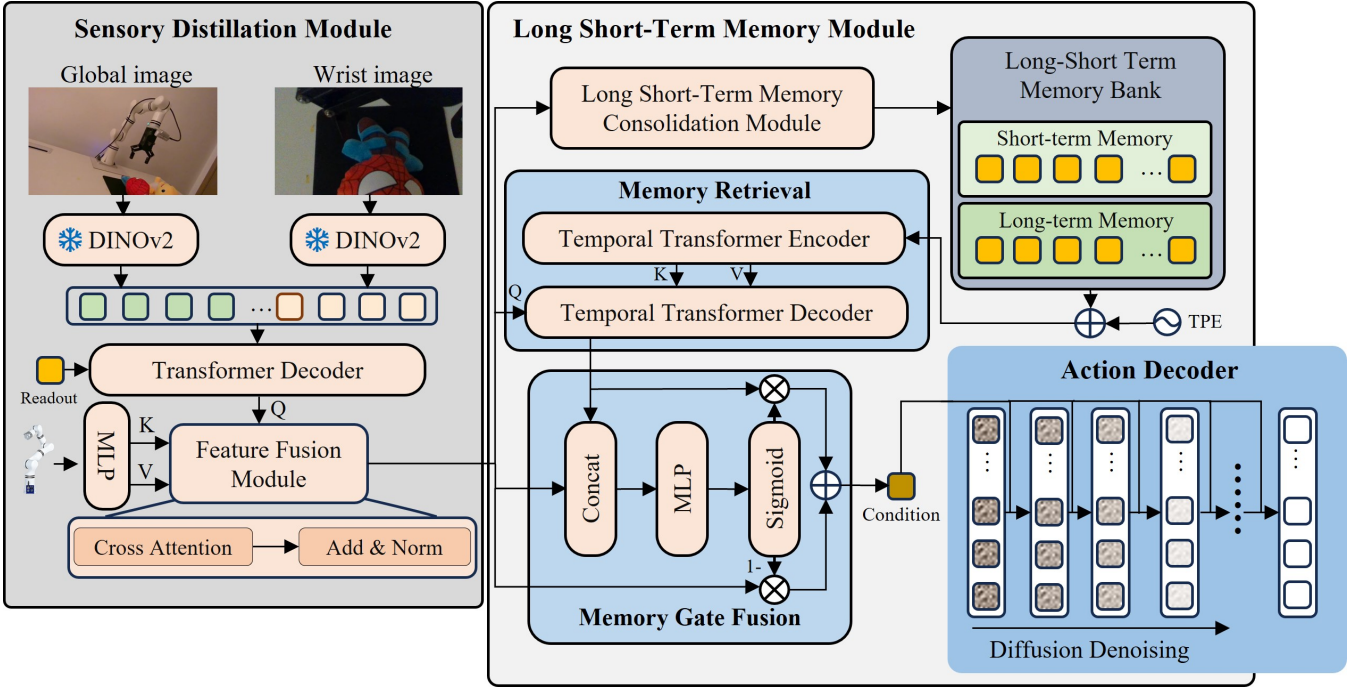


Fig. 2: **Overview of MemoAct architecture.** The sensory distillation module first encodes RGB images and proprioceptive states into high-fidelity features, termed sensory memory. This memory serves as a query to retrieve relevant historical context from the long short-term memory bank, which is processed by a temporal transformer encoder. Subsequently, a gating network adaptively fuses the retrieved history with the current sensory memory to produce a condition token. Guided by this token, the action decoder iteratively denoises random noise into history-aware action trajectories. Finally, the consolidation module updates the memory bank after each forward pass.

### B. History-Aware Robotic Manipulation Policies

To obtain historical perception capabilities, several approaches [13], [16]–[18] employ a fixed-size FIFO memory bank. Although effective for tasks with short-term dependencies, these methods struggle with long-horizon manipulation due to their limited context window. To increase the effective temporal span, MemoryVLA [10] moves beyond strict FIFO mechanisms by merging adjacent similar frames. However, this merging process risks discarding subtle yet essential cues required for precise decision-making, thereby impeding accurate task state tracking. MTIL [9] leverages the Mamba2 [31] architecture to compress the entire history into a fixed-size hidden state for efficient updates. Yet, such compression often leads to information loss, particularly when tasks demand the precise recall of distant historical context [32]. In this work, we propose a novel memory framework to reconcile these trade-offs, capable of retaining long-horizon retention while accurately tracking task states.

## III. METHOD

In this work, we propose MemoAct, which can be decomposed into three functions: a sensory distillation module  $f_{sdm} : O_t \rightarrow F_O^t$ , a long short-term memory module  $f_{lstm} : F_O^t, F_M^t \rightarrow F_C^t$ , and a memory-augmented action decoder  $f_{ad} : F_C^t \rightarrow A_{t:t+m-1}$ . The overall framework is illustrated in Fig. 2.

### A. Sensory Distillation Module for Extracting Sensory Memory

Given an RGB image  $I^t \in \mathbb{R}^{H \times W \times 3}$ , we first encode it into a patch-level feature map  $F_I^t \in \mathbb{R}^{P \times P \times C}$  using DINOv2 backbone [33] to capture rich semantic representations. Consistent with prevalent practices [9], [34], the parameters of DINOv2 are frozen during training. To mitigate information redundancy and reduce memory consumption, we introduce a dedicated transformer layer equipped with a single learnable readout token that queries the patch-level features to produce a compressed representation  $F_R^t \in \mathbb{R}^{1 \times C}$ . Simultaneously, the robot’s proprioceptive state  $S_t$  is projected into a latent embedding  $F_S^t \in \mathbb{R}^{1 \times C}$  via a Multilayer Perceptron (MLP), aligning its dimensionality with the visual token. To effectively synthesize these multi-modal inputs, we propose a Feature Fusion Module, formulated as:

$$F_O^t = \text{LN} \left( \text{Softmax} \left( \frac{(F_R^t W_Q) \cdot (F_S^t W_K)^T}{\sqrt{d_C}} \right) \cdot (F_S^t W_V) + F_R^t \right), \quad (1)$$

where the linearly transformed compressed visual token  $F_R^t$  serves as the query, while the projected state features  $F_S^t$  serve as both key and value. Through this attention mechanism, we derive the sensory memory  $F_O^t \in \mathbb{R}^{1 \times C}$ .

### B. Long Short-Term Memory Module for Temporal Modeling

**Long Short-Term Memory Bank.** Formally, we define the short-term memory bank (STMB) as  $M_S \in$

$\mathbb{R}^{T_s \times C}$ , with a maximum capacity of  $T_s = 6$ . Correspondingly, the long-term memory bank (LTMB) is denoted as  $M_L \in \mathbb{R}^{T_k \times C}$ , constrained by a maximum length of  $T_k = 8$ . We denote the collection of all tokens stored in both the STMB and LTMB as  $F_M^t$ .

**Memory Consolidation.** We propose a joint consolidation module that orchestrates the interaction between the distinct STMB and LTMB, as illustrated in Fig. 3. Upon the arrival of a new observation at time step  $t$ , the system first evaluates the STMB status. When the STMB reaches its capacity, the oldest  $N_{sc} = 3$  tokens are retrieved and augmented with learnable Temporal Positional Embeddings (TPE). We append a learnable summary token to this sequence and process it via a causal transformer encoder. Through this interaction, the summary token distills essential spatiotemporal features from the  $N_{sc}$  tokens. Finally, the updated summary token is transferred to the LTMB, and the original  $N_{sc}$  tokens are removed from the STMB to free up capacity.

When the LTMB reaches its capacity limit, we depart from the conventional FIFO eviction policy [13], [16], [17]. Instead, drawing inspiration from MemoryVLA [10], we compute the pairwise similarity between adjacent tokens and merge the two most similar entries.

This strategy significantly extends the temporal horizon retained in the LTMB while ensuring the STMB preserves lossless, high-fidelity information, thereby balancing accurate task-state tracking with robust long-horizon retention.

**Memory Retrieval and Gate Fusion.** To effectively capture the temporal dynamics of manipulation tasks, we introduce a transformer encoder-decoder architecture incorporating a causal attention mechanism. As illustrated in Fig. 2, the comprehensive memory context  $F_M^t$  is first augmented with learnable positional embeddings to preserve sequence order. This sequence is then processed by a temporal transformer encoder to model long-range dependencies. Subsequently, we employ a cross-attention mechanism where the current sensory memory  $F_O^t$  serves as the query to retrieve relevant historical information from the encoded context, yielding the retrieved feature  $F_{OR}^t$ . Finally, to balance immediate perception with historical context, both the retrieved feature  $F_{OR}^t$  and the original sensory memory  $F_O^t$  are fed into a gating network (as shown in Fig. 2). This module adaptively fuses the two representations to produce the final conditional token  $F_C^t$ , which guides the action decoder in generating history-aware trajectories.

### C. Conditional Diffusion-Based Action Decoder for Action Generation

We formulate the action generation process as a conditional denoising procedure. Specifically, the action decoder progressively eliminates noise sampled from a Gaussian distribution  $\mathcal{N}(0, \sigma^2 I)$  to reconstruct the clean action. Conditioned on the memory-augmented token

### Long Short-Term Memory Consolidation Module

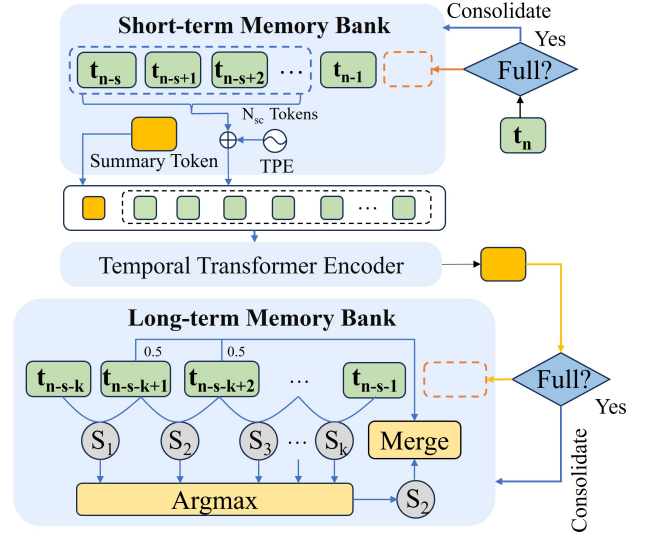


Fig. 3: **Illustration of the Long Short-Term Memory Consolidation Module.** Newly generated observation embeddings are first appended to the STMB. Upon saturation of the STMB capacity, the earliest  $N_{sc}$  entries are compressed by feeding them, alongside a learnable summary token, into the temporal transformer encoder. The resulting summary token is migrated to the LTMB, while the original  $N_{sc}$  entries are discarded. The most similar adjacent pair in the LTMB is merged to ensure storage efficiency.

$F_C^t$ , the denoising update at step  $k$  is defined as:

$$A_{k-1}^{t:t+m-1} = \alpha (A_k^{t:t+m-1} - \gamma \epsilon_\theta (F_C^t, A_k^{t:t+m-1}, k) + N(0, \sigma^2 I)), \quad (2)$$

where  $\epsilon_\theta$  denotes a UNet-based [35] noise predictor, while  $\alpha$  and  $\gamma$  serve as hyperparameters governing the diffusion schedule. In this work, we employ the DDPM [36] as our noise scheduler. Accordingly, the training objective minimizes the Mean Squared Error (MSE) between the predicted noise and the ground-truth noise  $\epsilon_k$ :

$$L_{\text{diff}} = \text{MSE} (\epsilon_\theta (F_C^t, A_k^{t:t+m-1}, k), \epsilon_k^{t:t+m-1}). \quad (3)$$

### D. Training

Diverging from the conventional practice of randomly sampling independent observation-action pairs  $\{(O_t, A_{t:t+m-1})\}$ , we adopt a streaming training paradigm to preserve temporal continuity. In this framework, each training batch is constructed exclusively from a single episode, with samples loaded in strict chronological order rather than being randomly shuffled. This ensures that the long short-term memory bank is populated sequentially, creating an ordered temporal context that is essential for effective model training. To address boundary conditions where the prediction horizon  $t + m - 1$  exceeds the trajectory length, we pad

the sequence by replicating the terminal time step. The detailed training procedure is outlined in Algorithm 1.

---

**Algorithm 1** MemoAct Training.

---

**Require:** Expert trajectories  $\mathcal{D} = \{\tau_i\}$ , where  $\tau_i = (O_1, A_1, \dots, O_{T_i}, A_{T_i})$ , Chunk size  $m$ , Batch size  $B$ , Optimizer  $Opt$ , Loss function  $\mathcal{L}$  (MSE) Sensory Distillation Module  $f_{sdm_{\theta_1}}$ , Long Short-Term Memory Bank  $LSTMB$ , Action Decoder  $f_{ad_{\theta_3}}$ , Long Short-Term Memory Module  $f_{lstm_{\theta_2}}$ ,

```

1: Initialize variables  $start = 0$ ,  $end = B$ , and policy
   parameters  $\theta_1, \theta_2, \theta_3$ .
2: for each training epoch do
3:   for each trajectory  $\tau_i \in \mathcal{D}$  do
4:      $X_{start:end-1} \leftarrow f_{sdm_{\theta_1}}(O_{start:end-1})$ 
5:      $\mathcal{L}_{batch} \leftarrow 0$ 
6:     for  $t = start$  to  $end - 1$  do
7:       # Memory Retrieval and Gate Fusion
8:        $C_t = f_{lstm_{\theta_2, forward}}(X_t, LSTMB)$ 
9:        $\mathcal{L}_t = \mathcal{L}(\epsilon_K^{t:t+m-1}, f_{ad_{\theta_3}}(C_t, k, A_K^{t:t+m-1}))$ 
10:      # Memory Consolidation
11:       $f_{lstm_{\theta_2, mcm}}(X_t.detach())$ 
12:       $\mathcal{L}_{batch} += \mathcal{L}_t$ 
13:    end for
14:     $\mathcal{L}_{batch}.mean().backward()$ 
15:    # Update parameters  $\theta_1, \theta_2, \theta_3$ 
16:     $Opt.step()$ 
17:     $start += B$ 
18:     $end += B$ 
19:  end for
20:   $start = 0$ 
21:   $end = B$ 
22:  Clear  $LSTMB$ 
23: end for
24: return Trained MemoAct.

```

---

#### IV. EXPERIMENTS

To comprehensively evaluate the performance of MemoAct, we designed a series of experiments to address the following three core research questions:

**(Q1)** How does MemoAct compare against state-of-the-art baselines on both simulated and real-world tasks?

**(Q2)** How does each individual module of MemoAct contribute to the overall performance?

**(Q3)** How do the capacities of the long-term and short-term memory banks influence the performance of MemoAct, and how should these parameters be selected?

**(Q4)** Can the long short-term memory module of MemoAct be seamlessly integrated into other baseline policies, and does it consistently yield performance improvements in history-aware tasks?

##### A. Experimental Setup

**Simulation Setup.** All simulations are conducted in RoboTwin 2.0 [22] with a Cobot Magic mobile manipu-

lator. Visual inputs are captured via an Intel RealSense L515 RGB-D camera for MemoryRTBench and a D435 RGB-D camera for RMBench.

**Real-robot Setup.** Our physical setup comprises a Realman RM65-B robotic arm with a TEK CTAG2F90-C gripper. For perception, we employ a global Intel RealSense D455 RGB-D camera and a wrist-mounted Intel RealSense D435 RGB-D camera.

**Tasks and Protocols.** To comprehensively evaluate task state tracking and long-horizon retention, we introduce MemoryRTBench, which consists of four simulation tasks. To ensure a thorough assessment, we also benchmark MemoAct on the language-independent tasks of RMBench, followed by validation on two real-world tasks (see Fig. 4 for details). These tasks are characterized by multiple subtasks and frequent occurrences of perceptually identical observations across different states, compelling the policy to rely on historical context for disambiguation. Moreover, their extended execution horizons require recalling the initial states of objects, posing a strict demand for robust long-term memory. During evaluation, we execute 50 trials per task for MemoryRTBench, 100 trials for RMBench, and 10 trials for real-world scenarios. For fairness, all policies share identical initialization states in every evaluation episode.

**Metrics.** Given that the tasks involve multiple sub-stages, we employ success rate as the primary metric to strictly measure performance differences. A trial is considered successful if and only if the robot sequentially completes all sub-tasks.

**Baselines.** First, we compare our method against two representative visuomotor policies: ACT [4] and Diffusion Policy (DP) [3]. Furthermore, to eliminate the confounding factors introduced by model scale and ensure a fair comparison, we extract the memory mechanisms from MemoryVLA [10] and SAM2Act [17] to construct two specific baselines:

- **MVMP (MemoryVLA Memory mechanism-enhanced Policy):** We construct a memory bank updated via similarity metrics. It utilizes a query mechanism to retrieve relevant history and employs a gating network to adaptively aggregate the retrieved information with current observations. The resulting features serve as condition tokens to guide action generation.
- **SAMP (SAM2Act Memory mechanism-enhanced Policy):** We implement a FIFO memory bank. It employs a query-based approach to retrieve historical memory tokens, which are subsequently utilized as condition tokens for action generation.

Crucially, apart from the specific memory modules, all other architectural components and training configurations for the two baselines remain identical to MemoAct.

##### B. Results

**Superiority of MemoAct over Baselines (Q1).** As presented in Tables I, II, and III, MemoAct demonstrates

MemoryRTBench Real-world Tasks

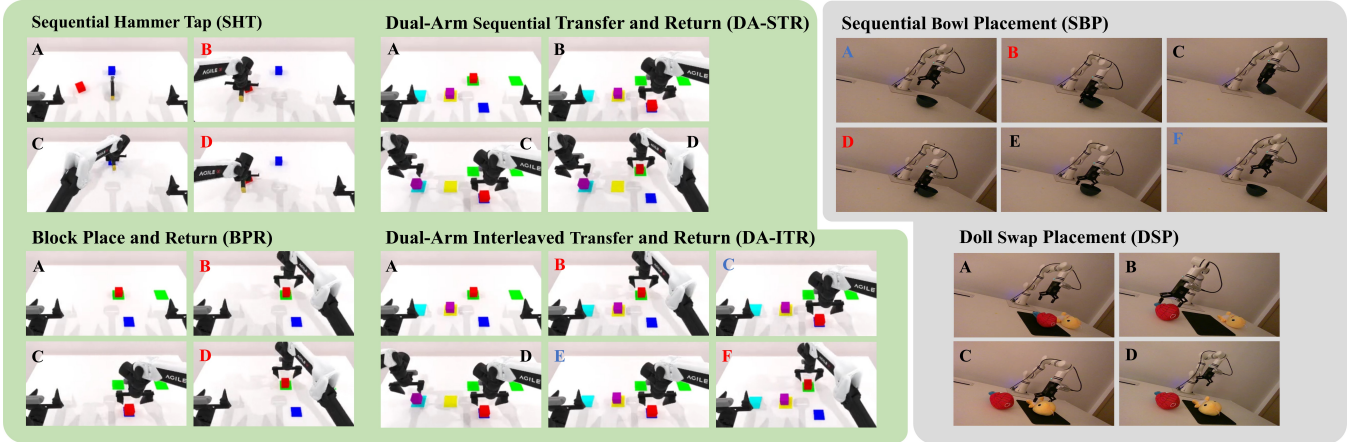


Fig. 4: Overview of simulation and real-world tasks. The figure illustrates four simulation tasks from MemoryRTBench alongside two additional real-world tasks, designed to evaluate the model’s capabilities in task state tracking and long-horizon retention. The tasks are executed sequentially following the alphabetical order (i.e., A → B → C → ...). Notably, identical observations encountered during the execution are highlighted in red or blue.

superior performance across all evaluated simulation and physical environments. It significantly outperforms the strongest baseline, MVMP, by margins of 24.5% in MemoryRTBench, 21.0% in RMBench, and 22.5% in real-world tasks.

We observe that methods lacking memory modules, specifically ACT and DP, struggle significantly. They yield average success rates of only 4.5% and 3% on MemoryRTBench, and similarly poor results (5.5% and 4.5%) on RMBench. Notably, DP’s success rate drops to 0% in real-world settings, confirming that historical context is indispensable for these tasks.

TABLE I: Performance comparison results of MemoAct and baseline methods on the MemoryRTBench.

Tasks \ Methods	ACT [4]	DP [3]	SAMP [17]	MVMP [10]	MemoAct (ours)
SHT	18%	12%	74%	44%	<b>86%</b>
BPR	0%	0%	60%	96%	<b>100%</b>
DA-STR	0%	0%	44%	56%	<b>100%</b>
DA-ITR	0%	0%	54%	92%	<b>100%</b>
Average	4.5%	3%	58%	72%	<b>96.5%</b>

TABLE II: Performance comparison results of MemoAct and baseline methods on the RMBench.

Tasks \ Methods	ACT [4]	DP [3]	SAMP [17]	MVMP [10]	MemoAct (ours)
Put Back Block	0%	0%	23%	34%	<b>41%</b>
Swap T	2%	16%	26%	<b>55%</b>	<b>55%</b>
Rearrange Blocks	20%	0%	47%	21%	<b>98%</b>
Observe and Pick Up	2%	2%	3%	4%	<b>4%</b>
Average	5.5%	4.5%	24.75%	28.5%	<b>49.5%</b>

For SAMP, while it executes sequential subtasks effectively in SHT, SBP, and DSP, it suffers from termination failures, often entering an erroneous loop after completing the final subtask. Furthermore, in tasks requiring long-horizon retention (e.g., BPR, DA-ITR, and Put Back Block), SAMP struggles to recall initial object states. We attribute this to its FIFO memory

TABLE III: Performance comparison results of MemoAct and baseline methods on real-world tasks.

Tasks \ Methods	DP [3]	SAMP [17]	MVMP [10]	MemoAct (ours)
SBP	0/10	6/10	8/10	<b>10/10</b>
DSP	0/10	2/10	5/10	<b>7/10</b>
Average	0/10	4/10	6.5/10	<b>8.75/10</b>

update mechanism, where incoming observations rapidly displace older data, causing a sharp decline in long-horizon retention capabilities.

Conversely, MVMP exhibits robust long-horizon retention, achieving competitive results in BPR, SBP, and even tying with MemoAct (55%) in Swap T task. However, in tasks demanding strict sequential tracking, such as SHT and Rearrange Blocks, MVMP frequently bypasses the immediate subtask to prematurely execute the subsequent one. Consequently, its performance in Rearrange Blocks drops to 21%, compared to MemoAct’s 98%. We hypothesize that while similarity-based memory updates effectively retain early history, they are prone to merging distinct temporal features, resulting in disordered subtask execution sequences.

These phenomena provided critical insights for MemoAct, motivating a memory framework that synergizes lossless short-term memory with persistent long-term memory. Nevertheless, limitations remain in fine-grained manipulation. For instance, in the Observe and Pick Up task, the presence of multiple objects makes it difficult for the robot to recall the precise location of the target, leading to task failure. We attribute this to the compression of all DINOv2 visual tokens into a single global token, which inevitably sacrifices fine-grained spatial precision.

### C. Ablation Studies

We further investigate the specific contributions of individual modules within MemoAct (Q2), as summarized in Table IV. First, replacing DINOv2 with ResNet-18 [37] causes an 18% drop in average success rate, highlighting DINOv2’s superior visual representation. Second, within the memory consolidation module, removing TPE or replacing the temporal transformer encoder with addition significantly degrades performance on the complex SHT task (dropping to 78% and 72%, respectively), proving that explicit temporal modeling is crucial for strict sequential execution. Finally, replacing the gating network with direct addition (Gate → Add) reduces SHT and DA-ITR performance, demonstrating the necessity of adaptive feature aggregation for integrating current and historical observations.

TABLE IV: Ablation experimental results evaluating different variants of MemoAct. “Consol. Temp. Enc.” refers specifically to the temporal transformer encoder within the long short-term memory consolidation module.

Variants \ Tasks	SHT	BPR	DA-STR	DA-ITR	Average
DINOv2 [33] → ResNet18 [37]	80%	64%	80%	90%	78.5%
w/o TPE	78%	100%	100%	100%	94.5%
Consol. Temp. Enc. → Add	72%	100%	100%	100%	93%
Gate → Add	82%	100%	100%	96%	94.5%
<b>MemoAct (ours)</b>	<b>86%</b>	<b>100%</b>	<b>100%</b>	<b>100%</b>	<b>96.5%</b>

The capacities of the long-term and short-term memory banks dictate long-horizon retention and task state tracking, respectively (Q3), as shown in Fig. 5. Reducing long-term capacity ( $T_k = 0$ ) severely degrades tasks requiring initial state recall (BPR, DA-STR, DA-ITR). Conversely, blindly expanding it ( $T_k = 12$ ) drops the average success rate to 91%, as excessive history introduces noisy and redundant features that interfere with decision-making.

For short-term memory, reducing capacity drastically impairs the SHT task (dropping to 46% at  $T_s = 2$ ) and causes repetitive or skipped sub-tasks in DA-ITR, proving its necessity for accurate state tracking. While further increasing short-term capacity beyond the baseline yields no performance drop, it incurs unnecessary memory and computational overhead. **Thus, we set  $T_k = 8$ ,  $T_s = 6$ , and  $N_{sc} = 3$  to optimally balance performance and efficiency (Q3).**

### D. Extension

The long short-term memory consolidation module (MCM) of MemoAct can be seamlessly integrated into existing baseline policies and consistently yields substantial performance improvements in history-aware tasks. (Q4) We integrated MCM into a representative baseline policy, DP3 [38]. As demonstrated in Table V, equipping DP3 with MCM leads to a dramatic enhancement in overall performance on MemoryRTBench, with the average success rate surging from 26% to 76.5%.

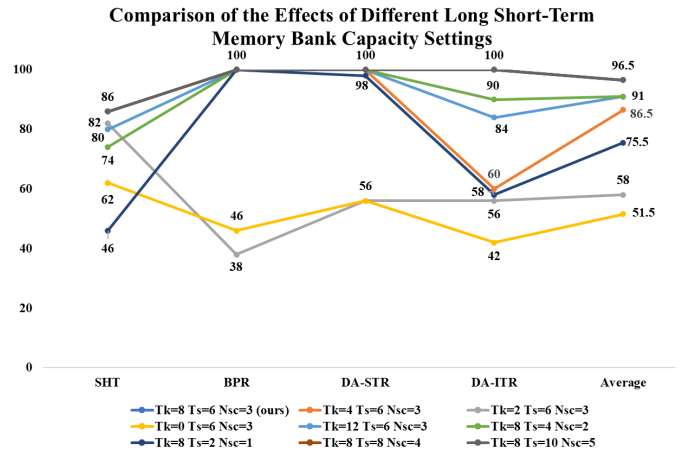


Fig. 5: Performance comparison of MemoAct under different memory capacities (%). Long-term memory primarily dictates long-horizon retention capabilities, whereas short-term memory is critical for maintaining accurate task state tracking.

TABLE V: Performance comparison between DP3 and DP3+MCM on MemoryRTBench. MCM denotes the long short-term memory consolidation module of MemoAct.

Methods \ Tasks	SHT	BPR	DA-STR	DA-ITR	Average
DP3 [38]	8%	46%	50%	0%	26%
<b>DP3 + MCM (Ours)</b>	<b>78%</b>	<b>100%</b>	<b>52%</b>	<b>76%</b>	<b>76.5%</b>

## V. CONCLUSIONS

Inspired by the Atkinson–Shiffrin memory model, we propose MemoAct, a novel visuomotor policy that transcends the limitations of the standard Markov assumption, endowing robots with precise task state tracking and robust long-horizon retention. Experiments across simulation and real-world settings demonstrate significant performance gains over existing methods. Despite these promising results, we acknowledge several limitations that outline directions for future research. First, compressing an entire RGB image into a single token via the sensory distillation module inevitably compromises visual fidelity. We plan to explore adaptive compression mechanisms that better balance memory storage efficiency with visual precision. Second, our method still relies on expanding the observation window to endow the model with historical awareness. Although it achieves long-horizon modeling to some extent, it cannot effectively exploit useful information outside the observation window. In future work, we aim to distill valuable historical knowledge into permanent, reusable experience for robots, thus enabling lifelong learning.

## REFERENCES

- [1] P. Intelligence, A. Amin, R. Aniceto, A. Balakrishna, K. Black, K. Conley, G. Connors, J. Darphinian *et al.*, “ $\pi_{0,6}^*$ : a vla that learns from experience,” 2025. [Online]. Available: <https://arxiv.org/abs/2511.14759>

- [2] R. Team, “Rdt2: Enabling zero-shot cross-embodiment generalization by scaling up umi data,” 2025.
- [3] C. Chi, Z. Xu, S. Feng, E. Cousineau, Y. Du, B. Burchfiel, R. Tedrake, and S. Song, “Diffusion policy: Visuomotor policy learning via action diffusion,” *The International Journal of Robotics Research*, vol. 44, no. 10-11, pp. 1684–1704, 2025.
- [4] T. Z. Zhao, V. Kumar, S. Levine, and C. Finn, “Learning fine-grained bimanual manipulation with low-cost hardware,” *arXiv preprint arXiv:2304.13705*, 2023.
- [5] J. BJORCK, F. Castañeda, N. Cherniadev, X. Da, R. Ding, L. Fan, Y. Fang, D. Fox, F. Hu, S. Huang *et al.*, “Gr00t n1: An open foundation model for generalist humanoid robots,” *arXiv preprint arXiv:2503.14734*, 2025.
- [6] B. Zitkovich, T. Yu, S. Xu, P. Xu, T. Xiao, F. Xia, J. Wu, P. Wohlhart, S. Welker, A. Wahid *et al.*, “Rt-2: Vision-language-action models transfer web knowledge to robotic control,” in *Conference on Robot Learning*. PMLR, 2023, pp. 2165–2183.
- [7] M. J. Kim, K. Pertsch, S. Karamcheti, T. Xiao, A. Balakrishna, S. Nair, R. Rafailov, E. Foster, G. Lam, P. Sankeki *et al.*, “Openvla: An open-source vision-language-action model,” *arXiv preprint arXiv:2406.09246*, 2024.
- [8] H. Li, Y. Zuo, J. Yu, Y. Zhang, Z. Yang, K. Zhang, X. Zhu, Y. Zhang, T. Chen, G. Cui *et al.*, “Simplevla-rl: Scaling vla training via reinforcement learning,” *arXiv preprint arXiv:2509.09674*, 2025.
- [9] Y. Zhou, Y. Lin, F. Peng, J. Chen, K. Huang, H. Yang, and Z. Yin, “Mtil: Encoding full history with mamba for temporal imitation learning,” *IEEE Robotics and Automation Letters*, 2025.
- [10] H. Shi, B. Xie, Y. Liu, L. Sun, F. Liu, T. Wang, E. Zhou, H. Fan, X. Zhang, and G. Huang, “Memoryvla: Perceptual-cognitive memory in vision-language-action models for robotic manipulation,” *arXiv preprint arXiv:2508.19236*, 2025.
- [11] Y. Dai, H. Fu, J. Lee, Y. Liu, H. Zhang, J. Yang, C. Finn, N. Fazeli, and J. Chai, “Robomme: Benchmarking and understanding memory for robotic generalist policies,” 2026. [Online]. Available: <https://arxiv.org/abs/2603.04639>
- [12] J. Chen, H. Fang, C. Wang, S. Wang, and C. Lu, “History-aware visuomotor policy learning via point tracking,” *arXiv preprint arXiv:2509.17141*, 2025.
- [13] M. Koo, D. Choi, T. Kim, K. Lee, C. Kim, Y. Seo, and J. Shin, “Hamlet: Switch your vision-language-action model into a history-aware policy,” *arXiv preprint arXiv:2510.00695*, 2025.
- [14] X. Liu, Y. Zhou, F. Weigend, S. Sonawani, S. Ikemoto, and H. B. Amor, “Diff-control: A stateful diffusion-based policy for imitation learning,” in *2024 IEEE/RSJ International Conference on Intelligent Robots and Systems (IROS)*. IEEE, 2024, pp. 7453–7460.
- [15] Q. Hu, Z. Qiu, Z. Xu, K. Zhang, X. Bu, Z. Sun, B. Zhang, J. Zhao, Z. Gan, and W. Ding, “Resolving state ambiguity in robot manipulation via adaptive working memory recoding,” *arXiv preprint arXiv:2512.24638*, 2025.
- [16] M. Lin, X. Liang, B. Lin, L. Jingzhi, Z. Jiao, K. Li, Y. Ma, Y. Liu, S. Zhao, Y. Zhuang, and X. Liang, “Echovla: Robotic vision-language-action model with synergistic declarative memory for mobile manipulation,” 2025. [Online]. Available: <https://arxiv.org/abs/2511.18112>
- [17] H. Fang, M. Grotz, W. Pumacay, Y. R. Wang, D. Fox, R. Krishna, and J. Duan, “Sam2act: Integrating visual foundation model with a memory architecture for robotic manipulation,” *arXiv preprint arXiv:2501.18564*, 2025.
- [18] H. Li, S. Yang, Y. Chen, Y. Tian, X. Yang, X. Chen, H. Wang, T. Wang, F. Zhao, D. Lin *et al.*, “Cronusvla: Transferring latent motion across time for multi-frame prediction in manipulation,” *arXiv preprint arXiv:2506.19816*, 2025.
- [19] R. C. Atkinson and R. M. Shiffrin, “Human memory: A proposed system and its control processes,” in *Psychology of learning and motivation*. Elsevier, 1968, vol. 2, pp. 89–195.
- [20] E. Tulving *et al.*, “Episodic and semantic memory,” *Organization of memory*, vol. 1, no. 381-403, p. 1, 1972.
- [21] A. Baddeley, “Working memory: An overview,” *Working memory and education*, pp. 1–31, 2006.
- [22] T. Chen, Z. Chen, B. Chen, Z. Cai, Y. Liu, Z. Li, Q. Liang, X. Lin, Y. Ge, Z. Gu *et al.*, “Robotwin 2.0: A scalable data generator and benchmark with strong domain randomization for robust bimanual robotic manipulation,” *arXiv preprint arXiv:2506.18088*, 2025.
- [23] T. Chen, Y. Wang, M. Li, Y. Qin, H. Shi, Z. Li, Y. Hu, Y. Zhang, K. Wang, Y. Chen *et al.*, “Rmbench: Memory-dependent robotic manipulation benchmark with insights into policy design,” *arXiv preprint arXiv:2603.01229*, 2026.
- [24] M. Song, X. Deng, Z. Zhou, J. Wei, W. Guan, and L. Nie, “A survey on diffusion policy for robotic manipulation: Taxonomy, analysis, and future directions,” *Authorea Preprints*, 2025.
- [25] R. Firoozi, J. Tucker, S. Tian, A. Majumdar, J. Sun, W. Liu, Y. Zhu, S. Song, A. Kapoor, K. Hausman *et al.*, “Foundation models in robotics: Applications, challenges, and the future,” *The International Journal of Robotics Research*, vol. 44, no. 5, pp. 701–739, 2025.
- [26] B. Ai, S. Tian, H. Shi, Y. Wang, T. Pfaff, C. Tan, H. I. Christensen, H. Su, J. Wu, and Y. Li, “A review of learning-based dynamics models for robotic manipulation,” *Science Robotics*, vol. 10, no. 106, p. eadt1497, 2025.
- [27] S. Liu, L. Wu, B. Li, H. Tan, H. Chen, Z. Wang, K. Xu, H. Su, and J. Zhu, “Rdt-1b: a diffusion foundation model for bimanual manipulation,” *arXiv preprint arXiv:2410.07864*, 2024.
- [28] Y. Su, X. Zhan, H. Fang, Y.-L. Li, C. Lu, and L. Yang, “Motion before action: Diffusing object motion as manipulation condition,” *IEEE Robotics and Automation Letters*, 2025.
- [29] Q. Zhao, Y. Lu, M. J. Kim, Z. Fu, Z. Zhang, Y. Wu, Z. Li, Q. Ma, S. Han, C. Finn *et al.*, “Cot-vla: Visual chain-of-thought reasoning for vision-language-action models,” in *Proceedings of the Computer Vision and Pattern Recognition Conference*, 2025, pp. 1702–1713.
- [30] F. Zhu, Z. Yan, Z. Hong, Q. Shou, X. Ma, and S. Guo, “Wmpo: World model-based policy optimization for vision-language-action models,” *arXiv preprint arXiv:2511.09515*, 2025.
- [31] T. Dao and A. Gu, “Transformers are smms: Generalized models and efficient algorithms through structured state space duality,” *arXiv preprint arXiv:2405.21060*, 2024.
- [32] K. Wen, X. Dang, and K. Lyu, “Rnns are not transformers (yet): The key bottleneck on in-context retrieval,” *arXiv preprint arXiv:2402.18510*, 2024.
- [33] M. Oquab, T. Darcet, T. Moutakanni, H. Vo, M. Szafraniec *et al.*, “Dinov2: Learning robust visual features without supervision,” *arXiv preprint arXiv:2304.07193*, 2023.
- [34] Y. Zhong, X. Huang, R. Li, C. Zhang, Z. Chen, T. Guan, F. Zeng, K. N. Lui, Y. Ye, Y. Liang *et al.*, “Dexgraspvla: A vision-language-action framework towards general dexterous grasping,” *arXiv preprint arXiv:2502.20900*, 2025.
- [35] O. Ronneberger, P. Fischer, and T. Brox, “U-net: Convolutional networks for biomedical image segmentation,” in *International Conference on Medical image computing and computer-assisted intervention*. Springer, 2015, pp. 234–241.
- [36] J. Ho, A. Jain, and P. Abbeel, “Denosing diffusion probabilistic models,” *Advances in neural information processing systems*, vol. 33, pp. 6840–6851, 2020.
- [37] K. He, X. Zhang, S. Ren, and J. Sun, “Deep residual learning for image recognition,” in *Proceedings of the IEEE conference on computer vision and pattern recognition*, 2016, pp. 770–778.
- [38] Y. Ze, G. Zhang, K. Zhang, C. Hu, M. Wang, and H. Xu, “3d diffusion policy: Generalizable visuomotor policy learning via simple 3d representations,” in *Proceedings of Robotics: Science and Systems (RSS)*, 2024.